

Models for High-Energy Radiation from Blazars

G. E. Romero^{1,*} & M. M. Reynoso²

¹*Instituto Argentino de Radioastronomía (CCT La Plata - CONICET), C.C. N°5 (1894), Villa Elisa, Buenos Aires, Argentina.*

²*Instituto de Investigaciones Físicas (CONICET-UNMDP), Funes 3350, (7600) Mar del Plata, Buenos Aires, Argentina.*

**e-mail: romero@iar-conicet.gov.ar*

Abstract. We discuss on the modelling of blazar jets as emitters of multiwavelength radiation with the implementation of a lepto-hadronic treatment. Assuming that injection of non-thermal electrons and protons can take place at the base of the jet, the stationary particle distributions can be found using an inhomogeneous one-dimensional transport equation with cooling and convection. The goal of this approach is to replace the widely used one-zone purely leptonic approximation by a more realistic model. We argue that the rapid variability observed in emission from blazars can be obtained as a result of interaction of the jet with obstacles, i.e., molecular clouds and stars. Long term variability is likely related to changes in the injection and physical conditions in the acceleration region.

Key words. Blazars—radiation mechanisms: non-thermal—jets.

1. Introduction

The unification paradigm for Active Galactic Nuclei (AGN) suggests that different observational properties of these objects are basically due to the different angles of observations (e.g., Urry & Padovani 1995). Blazars are the AGN in which the jet direction makes a small angle with the line-of-sight. They come in two flavors, one where the synchrotron part of the spectrum peaks at low energies (LBLs) and the other with the peak at X-rays (XBL). The parent populations are FR II and FR I radio galaxies, respectively. The former are intrinsically more powerful sources, with higher accretion rates and more luminous jets. In what follows we will present a broadband jet model for both types of objects.

2. Basic scenario: The jet

We assume that the jet is launched from the black hole's ergosphere, being completely formed at a distance $z_0 = 50R_g$, and with a given initial bulk Lorentz factor Γ_0 . We assume that equipartition holds between the magnetic and kinetic energy at the base of the jet. This is required if the plasma is set in motion by magneto-centrifugal effects. The kinetic power is given by $L_j^{(\text{kin})} = \frac{q_j}{2} L_{\text{Edd}}$, where L_{Edd} is the

Eddington luminosity and $0 < q_j < 1$ is a numerical factor. The jet is modelled as a cone with an half-opening angle ξ . Most of its content is thermal plasma. The value of the magnetic field at the position z_0 in the jet is

$$B_0 = \sqrt{\frac{8L_j^{(\text{kin})}}{[r_j(z_0)]^2 v_b}}, \quad (1)$$

where $r_j(z_0) = z_0 \tan \xi$ is the jet radius at z_0 .

The jet magnetic energy is gradually converted into bulk kinetic energy and the field decreases as the flow accelerates. This is parametrized by:

$$B(z) = B_0 \left(\frac{z_0}{z}\right)^m, \quad (2)$$

with $m \in \{1, 2\}$. If all the magnetic energy is transformed into bulk kinetic energy, the Lorentz factor of the jet increases with z approximately as:

$$\Gamma_b(z) \approx 1 + \frac{B_0^2 z_0^2 \tan^2 \xi}{8\dot{m}_j c} \left[2 - \left(\frac{z_0}{z}\right)^{2m-2} \right].$$

In turn, a fraction q_{rel} of the bulk kinetic power is transformed into highly relativistic particles in a region that starts at z_{acc} . There the bulk kinetic energy is well below the magnetic one (sub-partition condition), and shocks can develop. Both primary electrons and protons are assumed to be injected at z_{acc} , over a length Δz along the jet, with a power law distribution in the frame of the jet,

$$Q'_{e,p}(z', E') = \frac{K_{e,p}}{4\pi} \left(\frac{z'_{\text{acc}}}{z'}\right) \left(\frac{E'}{m_i c^2}\right)^{-s} e^{-E'/E'_{\text{max}}}, \quad (3)$$

in units of $\text{GeV}^{-1} \text{s}^{-1} \text{cm}^{-3} \text{sr}^{-1}$.

The constants $K_{e,p}$ are fixed by normalizing the injected power as:

$$L'_{e,p} = \int_{V'} dV' \int_{E'_{\text{min}}} dE' E' Q'(z', E'). \quad (4)$$

The acceleration mechanism might be a diffusive shock acceleration (e.g., Drury 1983), but other possibilities like magnetic reconnection (de Gouveia Dal Pino *et al.* 2010) or the converter mechanism (Derishev *et al.* 2008) cannot be ruled out.

The maximum energies of the injected particles are determined from the balance between the acceleration rate and the cooling rates. The proton-to-electron ratio at the injection point is given by the parameter $a = L'_p/L'_e$ where $L'_e + L'_p = q_{\text{rel}} L_j^{(\text{kin})}$.

The main cooling processes are synchrotron emission for electrons and protons, and pp , $p\gamma$ interactions and adiabatic cooling for protons. Inverse Compton (IC) interactions with synchrotron photons in the jet are also considered. For the set of parameters of Table 1, we show the obtained cooling rates for electrons and protons at the position z_{acc} in the jet in Fig. 1. The acceleration rate with an efficiency η is also shown in the plot. The expression is: $t_{\text{acc}}^{-1} = \eta c e B'(z)/E'$. For other rates the reader can refer to Romero & Vila (2008) and Vila & Romero (2010).

Table 1. Parameters used.

Parameter	Value
M_{bh} : black hole mass	$1 \times 10^9 M_{\odot}$
d : distance	250 Mpc
$L_j^{(\text{kin})}$: jet kinetic power	$9.4 \times 10^{45} \text{erg s}^{-1}$
$\Gamma_b^{(0)}$: jet's bulk Lorentz factor at z_0	8
θ : viewing angle	2°
ξ_j : jet's half-opening angle	1°
q_{rel} : jet's content of relativistic particles	0.1
a : hadron-to-lepton power ratio	10, 10^3
q_m : magnetic to kinetic energy ratio at z_{acc}	0.38
z_0 : jet's launching point	$50 R_g$
z_{acc} : injection point	$91 R_g$
Δz : size of injection zone	$z_{\text{acc}} \tan \xi_j$
m : index for magnetic field dependence on z	1.8
s : spectral index injection	2.1
η : acceleration efficiency	10^{-6}
$E_p^{(\text{min})}$: minimum proton energy	3 GeV
$E_e^{(\text{min})}$: minimum electron energy	0.1 GeV

The steady-state particle distributions $N'_i(E, z)$ in the jet can be found by solving a 1-dimensional transport equation with cooling and convection along the jet, with a bulk velocity $v \approx c$:

$$v \frac{\partial N'_i}{\partial z} + \frac{\partial [b_i(z, E) N'_i]}{\partial E} + \frac{N'_i}{T_{\text{dec}}(E)} = Q'_i(z, E). \quad (5)$$

This equation is solved first for electrons, assuming no IC cooling. This first approximation to $N'_e(z, E)$ is then iteratively improved taking into account also the IC cooling rate t_{IC}^{-1} to solve the transport equation. The distribution of protons is

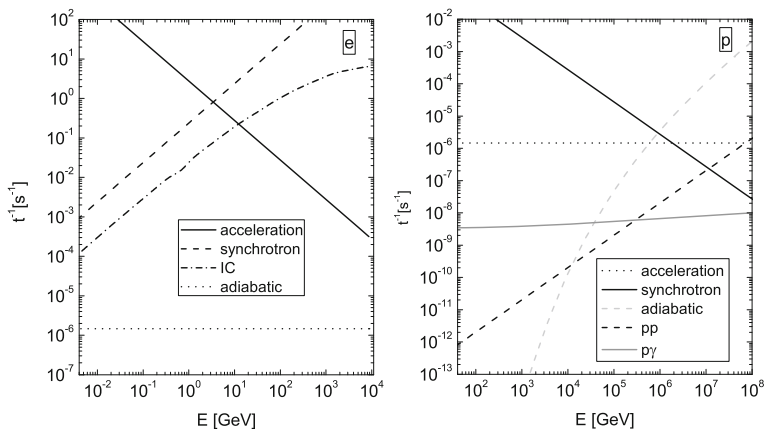


Figure 1. Acceleration and cooling rates for electrons (left panel) and protons (right panel). They are evaluated at a distance $z = z_{\text{acc}}$ from the central black hole.

obtained considering the cooling through $p\gamma$ interactions with the low energy photons in the jet. These inelastic interactions, together with the pp collisions, give rise to pions and their decay products, which include muons and neutrinos. The injection of pions $Q'_\pi(z, E)$ can be worked out using the proton distribution $N'_p(z, E)$ as in Reynoso & Romero (2009), applying the expressions of Lipari *et al.* (2007). The distribution of pions $N'_\pi(z, E)$ found with equation (5) is then considered to obtain the injection of muons $Q'_\mu(z, E)$, which in turn is used to obtain the muon distribution $N'_\mu(z, E)$. The different particle species are responsible for the radiative processes described in the next section.

3. Radiative processes

The relevance of different radiative processes can be appreciated from Fig. 1 for the example case with $a=10$. It can be seen that synchrotron emission of electrons is very important. IC emission, on the contrary, is weak. This justifies the approach used to solve the equations by decoupling them.

In the jet frame, where the particle distributions are isotropic, the synchrotron emissivity is

$$Q'_{\gamma,\text{syn}}(E'_\gamma, z') = \frac{\varepsilon'_{\text{syn}}(E'_{\text{ph}}, z')}{4\pi E'_\gamma}, \quad (6)$$

where $\varepsilon'_{\text{syn}}$ is the power per unit energy per unit volume of the synchrotron photons,

$$\varepsilon'_{\text{syn}}(E'_{\text{ph}}, z') = \left(\frac{1 - e^{-\tau_{\text{SSA}}(E'_{\text{ph}}, z')}}{\tau_{\text{SSA}}(E'_{\text{ph}}, z')} \right) \int_{E'_e}^{\infty} dE' 4\pi P_{\text{syn}} N'_e(E', z'). \quad (7)$$

Here, P_{syn} is the usual synchrotron power per unit energy emitted by the electrons. The effect of synchrotron self-absorption (SSA) within the jet is determined by an optical depth

$$\tau_{\text{SSA}}(E'_{\text{ph}}, z') = \int_0^{\frac{r_1(z')}{\sin\theta'}} dl' \alpha_{\text{SSA}}(E'_{\text{ph}}, z', l').$$

θ' is the viewing angle in the jet frame, and the SSA coefficient α_{SSA} is evaluated with its standard expression along the path in the jet. The IC emissivity is

$$Q'_{\gamma,\text{IC}}(E'_\gamma, z') = \frac{r_0^2 c}{2} \int_{E'_{\text{ph}}^{(\min)}}^{E'_\gamma} dE'_{\text{ph}} \frac{n'_{\text{ph}}(E'_{\text{ph}}, z')}{E_{\text{ph}}} \int_{E'_{\text{min}}}^{E'_{\text{max}}} dE' \frac{N'_e(E', z')}{\gamma_e^2} F(q), \quad (8)$$

where we integrate in the target photon energy E'_{ph} and in the electron energies E' between

$$E'_{\text{min}} = \frac{E'_\gamma}{2} + \frac{m_e c^2}{2} \sqrt{\frac{E'_\gamma}{2E'_{\text{ph}}} + \frac{E'^2_\gamma}{2m_e^2 c^4}} \quad \text{and} \quad E'_{\text{max}} = \frac{E'_\gamma}{1 - (E'_\gamma/E'_{\text{ph}})}. \quad (9)$$

As for the emission of protons, the relevant processes are pp and $p\gamma$ interactions. The gamma-ray emissivity is

$$Q'_{\gamma,pp}(E'_\gamma, z') = n'_c(z')c \int_0^1 \frac{dx}{x} N'_p \left(\frac{E'_\gamma}{x}, z' \right) \times F_\gamma \left(x, \frac{E'_\gamma}{x} \right) \sigma_{pp}^{(inel)} \left(\frac{E'_\gamma}{x} \right), \quad (10)$$

where the function $F_\gamma(x, E')$ is the same as defined by Kelner *et al.* (2006), for a proton energy $E' = E'_\gamma/x$. The target-proton density in the jet frame is $n'_c(z') = n_c(z'\Gamma_b)/\Gamma_b$. Its value in the observer frame is

$$n_c(z) = \frac{(1 - q_{\text{rel}})\dot{m}_j}{m_p \pi z^2 \tan^2 \xi_j v_b(z)}. \quad (11)$$

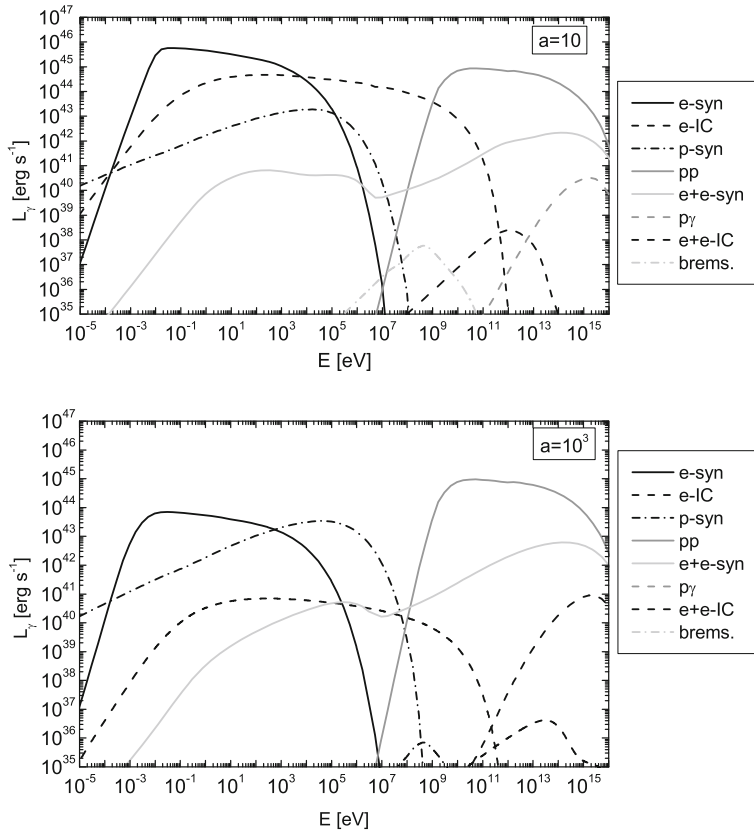


Figure 2. Spectral photon distribution for $a = 10$ in the upper panel and $a = 10^3$ in the lower one. The rest of the parameters take the values presented in Table 1.

4. Spectral energy distributions

In Fig. 2, we present two examples of spectral energy distributions (SEDs) obtained with our model. In the figure we plot L_γ , which is calculated as:

$$L_\gamma = 4\pi \int_V dV E_\gamma Q_\gamma(E_\gamma, z),$$

where the photon emissivity $Q_\gamma(E_\gamma, z)$ corresponds to the observer frame. The parameter $a = L'_p/L'_e$ takes the values 10 and 10^3 in different panels of Fig. 2. The main contributions arise from synchrotron emission of electrons, inelastic pp collisions and synchrotron radiation of secondary electron–positron pairs. The role of internal absorption, not included here, is discussed by Reynoso *et al.* (2011).

5. Variability

The particle distributions described here correspond to a steady-state jet. Temporal variability can be introduced in different forms according to the time scales involved:

- (1) For long time scales (days or more), with a time-dependent injection $Q'_i(z, E, t)$ and a time-derivative term $\partial N'/\partial t$ in the transport equation.
- (2) For short time scales (hours or less), through the entrainment of magnetized clouds or stars in the jet as proposed by Araudo *et al.* (2010), or by bends or turbulence produced through instabilities (Romero 1995).

Acknowledgements

We thank M. C. Medina for very useful discussions. This research was supported by CONICET (Argentina) through grants PIP 112-200901-00078 and PIP 112-200801-00587.

References

- Araudo, A. T., Bosch-Ramon, V., Romero, G. E. 2010, *Astron. Astrophys.*, **522**, id.A97.
 de Gouveia Dal Pino, E. M., Piovezan, P. P., Kadowaki, L. H. S. 2010, *Astron. Astrophys.*, **518**, id.A5.
 Derishev, E. V., Aharonian, F. A., Kocharovsky, V. V., Kocharovsky, Vl. V. 2008, *Int. J. Mod. Phys.*, **D17**, 1839.
 Drury, L. Oc. 1983, *Reps. Progr. Phys.*, **46**, 973.
 Kelner, S. R., Aharonian, F. A., Bugayov, V. V. 2006, *Phys. Rev.*, **D74**, 034018.
 Lipari, P., Lusignoli, M., Meloni, D. 2007, *Phys. Rev.*, **D75**, 123005.
 Reynoso, M. M., Romero, G. E. 2009, *Astron. Astrophys.*, **493**, 1.
 Reynoso, M. M., Medina, M. C., Romero, G. E. 2011, *Astron. Astrophys.*, **531**, A30.
 Romero, G. E., Vila, G. S. 2008, *Astron. Astrophys.*, **485**, 623.
 Romero, G. E. 1995, *Astrophys. Space Sci.*, **234**, 49.
 Vila, G. S., Romero, G. E. 2010, *Mon. Not. R. Astron. Soc.*, **403**, 1457.
 Urry, C. M., Padovani, P. 1995, *Publ. Astron. Soc. Pacific*, **107**, 803.